New emerging surface treatment of GFRP Hybrid bar for stronger durability of concrete structures

Cheolwoo Park[1a], Younghwan Park[2b], Seungwon Kim[1c] and Minkwan Ju[*1]

[1]*Department Of Civil Engineering, Kangwon National University, 346 Joongang-ro, Samcheok-si, Kangwon, 25913, Korea*
[2]*Division of Structural Engineering Research, Korea Institute of Construction Technology, 315 Goyang-dae-ro, Ilsan-seo-gu, Goyang-si, Gyenggi-Do, 10223, Korea*

Abstract. In this study, an innovative and smart glass fiber-reinforced polymer (GFRP) hybrid bar was developed for stronger durability of concrete structures. As comparing with the conventional GFRP bar, the smart GFRP Hybrid bar can promise to enhance the modulus of elasticity so that it makes the cracking reduced than the case when the conventional GFRP bar is used. Besides, the GFRP Hybrid bar can effectively resist the corrosion of conventional steel bar by the GFRP outer surface on the steel bar. In order to verify the bond performance of the GFRP Hybrid bar for structural reinforcement, uniaxial pull-out test was conducted. The variables were the bar diameter and the number of strands and pitch of the fiber ribs. Tensile tests showed a excellent increase in the modulus of elasticity, 152.1 GPa, as compared to that of the pure GFRP bar (50 GPa). The stress–strain curve was bi-linear, so that the ductile performance could be obtained. For the bond test, the entire GFRP Hybrid bar test specimens failed in concrete splitting due to higher shear strength resulting in concrete crushing as a function of bar deformation. Investigation revealed that an increase in the number of strands of fiber ribs enhanced the bond strength, and the pitch guaranteed the bond strength of 19.1 mm diameter hybrid bar with 15.9 mm diameter of core section of deformed steel bar specimens may be around 13.4 mm. For a comparative study using two representative code equations, the ACI 440 1R-15 equation is regarded as more suitable for predicting the bond strength of GFRP Hybrid bars, whereas the CSA S806-12 prediction is considered too conservative and is largely influenced by the bar diameter. For further study, various geometrical and material properties such as concrete cover, cross-sectional ratio, and surface treatment should be considered.

Keywords: GFRP Hybrid bar; durability; modulus of elasticity; bond test; code equations

1. Introduction

There has been wide interest in the use of glass fiber-reinforced polymer (GFRP) bars as possible replacements for reinforced steel bars in concrete structures. The high strength-to-weight ratio, corrosion resistance, and ease of handling in construction are apparent advantages as an

∗Corresponding author, Research Professor, E-mail: j_dean21@naver.com
[a] Professor, E-mail: tigerpark@kangwon.ac.kr
[b] Ph.D., E-mail: yhpark@kict.re.kr
[c] Ph.D. Candidate, E-mail: inncoms@naver.com

alternative construction material. Moreover, GFRP bars are more cost effective than other FRP bars such as carbon or aramid. In North America, many studies using FRP bars have been carried out in the field, and there are specified guidelines for the design and construction of reinforced concrete using FRP bars (ACI Committee 440, 2015, AASHTO, 2009, CAN/CSA S806, 2012).

GFRP bars have a lower modulus of elasticity than conventional steel bars, whereas the tensile strength is much higher. This lower modulus of elasticity of GFRP bars has been addressed in evaluating the serviceability in terms of deflection and crack width under flexural behavior. There have been some efforts toward hybrid installation of GFRP and steel bar to enhance the structural stiffness of members. Hybrid GFRP/steel-reinforced concrete members exhibit good ductility, serviceability, and load-carrying capacity. Qu *et al*. (2009) found that a proposed model for predicting deflection showed good accordance with the test results. There was also a report about the contribution of steel reinforcement for improving the flexural ductility of a member reinforced with a GFRP bar (Lau and Pam 2010).The hybrid reinforcing system, which is an artificial reinforcing method, may be a good alternative for improving the structural stiffness of a member reinforced a pure GFRP bar, although the design and construction details should be carefully examined. A hybrid reinforcing system (HRS) is fabricated by wrapping glass or carbon fiber around a core of plain steel or aluminum. The purpose of developing the hybrid bar is to enhance the capacity and ductility of reinforced concrete (RC) slabs. HRSs show a remarkable increase in the ultimate load capacity and ductility (Etman 2011).

In this study, an innovative and smart GFRP Hybrid bar with a deformed steel bar core and GFRP as an outer surface was developed for improved durability of concrete structures. It is thought that the hybrid GFRP bar could enhance the modulus of elasticity, thus reducing the cracking that occurs when a conventional GFRP bar is used. The hybrid bar can provide sufficient structural stiffness, effectively and smartly enhancing the serviceability performance. A deformed steel bar wrapped in GFRP also resists delamination of GFRP under bond stress due to mechanical interlocking caused by presence of steel ribs. To apply these new GFRP Hybrid bars to concrete members in the field, the bond strength should be experimentally verified. Generally, the bond behavior between concrete and a reinforcing steel bar can be considered constant and perfect; however, this is not valid for GFRP bars due to its lower modulus of elasticity as compared to conventional steel bars. This lower modulus of elasticity causes increased slip at the loaded end (Pecce *et al*. 2001). Many studies about the bond strength of GFRP bars have been performed, and it was found that the bond behavior was influenced by geometric and material-related factors (Tighiouart *et al.* 2005, Tastani and Mazaheripour *et al.* 2013, Xue *et al.* 2014, Islam *et al.* 2015).

The current paper presents both experimental and analytical investigation of the bond performance of the new hybrid GFRP bar. The parameters thought to have an influence on bond performance are the diameter of the bar, the number of strands in the fiber ribs, and rib spacing. Three identical specimens for each test variable were fabricated and direct pull-out tests were conducted. The experimental data were compared to the results of the ACI 440 1R-15 design equation and analytical boundaries for the new GFRP Hybrid bar were investigated.

2. Description of the new GFRP Hybrid bar

The proposed GFRP Hybrid bar was fabricated by a typical pultrusion thermosetting process used for most FRP bars. The noticeable difference as compared to conventional FRP bars is that the core section was made of deformed steel. Longitudinal fiber strands bound together with a

thermosetting vinyl ester resin was applied on the outer surface of the deformed steel bar. Fig. 1 illustrates the sections of the GFRP Hybrid bar. The core deformed steel bar is wrapped with GFRP and fiber ribs form on the surface of the GFRP. The GFRP is composed of 37.0% of E-glass fiber (by weight) in a vinyl ester resin.
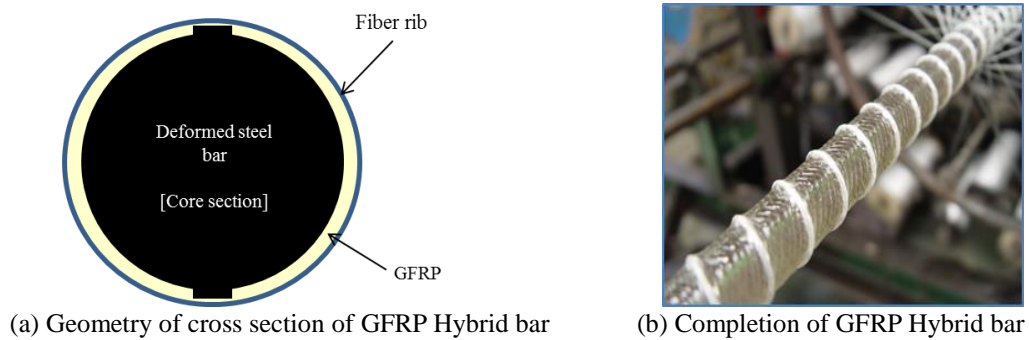

(a) Geometry of cross section of GFRP Hybrid bar   (b) Completion of GFRP Hybrid bar

Fig. 1 Sectional property of GFRP Hybrid bar and surface detail

(a) Impregnation process of glass fiber

(b) Fabrication of the hybrid section and thermosetting process
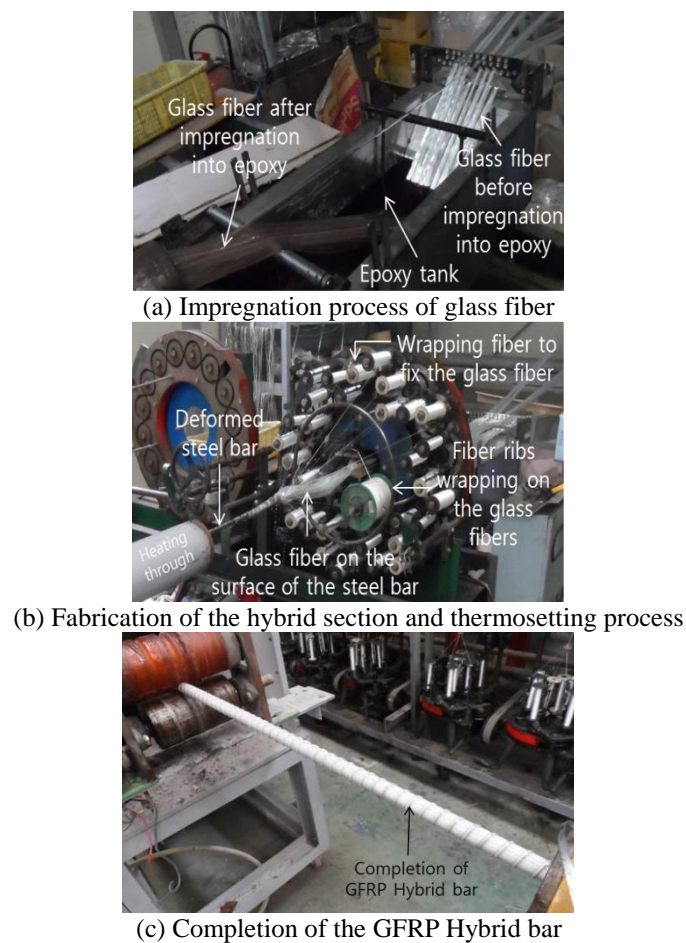

(c) Completion of the GFRP Hybrid bar

Fig. 2 Pultrusion process of GFRP Hybrid bar

The pitch of the fiber ribs, seen from the side view, was also a test variable. Fig. 2 shows the fabrication process. Fig. 2(a) shows the typical impregnation of glass fibers in an epoxy tank. After this process, the impregnated glass fibers were wrapped on the deformed steel bar by the pultrusion process. Simultaneously, the fiber winding equipment was used to form the ribs according to the designed pitch. The wet bar was passed through a heating tunnel to complete the GFRP Hybrid bar.

3. Description of the new GFRP Hybrid bar

3.1 Test specimens

The test variables were the diameter, number of strands of the fiber ribs, and the pitch of the fiber ribs. The anchorage concrete block was $200 \times 200 \times 200$ mm and the bond length was set as $5d_b$ (where d_b is the bar diameter), in compliance with ASTM D 7913. All of the bars were configured in the center of the anchorage concrete block. For the debonding section, waterproof sponge tube was inserted into the concrete. The detail of test specimen was shown in Fig. 3. Table 1 summarizes the average nominal diameter and geometrical properties of the GFRP Hybrid bar. To obtain the nominal diameter of a smooth bar, ASTM D 3916 specifies measuring the nominal diameter at several points along the length of the bar. For a ribbed GFRP bar, however, this method is impractical because of the variation in cross-sectional dimensions. A better approach is to calculate the average diameter from the mass, length, and density of a representative portion of the bar (Castro and Carino 1998). In this study, a immersing test was carried out and, the density and weight per unit length of GFRP Hybrid bars with lengths from 158 to 221 mm were measured. The calculated nominal diameter of the GFRP Hybrid bar was then used to calculate the bond strength of the test specimens. The average cross-sectional ratios of D19 (D16), D25 (D19), and D29 (D22) were calculated to be 0.71, 0.59, and 0.63, respectively. The cross-sectional ratios for the outer GFRP therefore ranged from 29–41%.
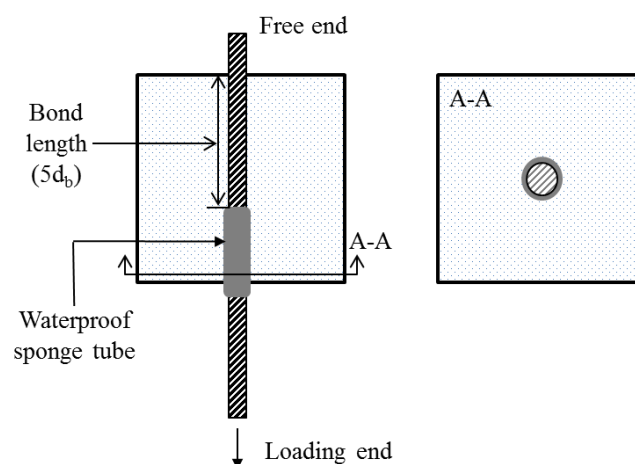

Fig. 3 Details of test specimen

Table 1 Average nominal diameter and geometrical properties of GFRP Hybrid bar

	Core diameter (mm)	Ave. nominal diameter of the hybrid bar (mm)	Gross area $(mm^2)^a$	Cross sectional area of steel $(mm^2)^b$	Ave. cross sectional ratio (b/a)
D19 (D16)[*]	15.9	18.9±0.2	280.6	198.6	0.71
D25 (D19)	19.1	24.9±0.2	487.0	286.5	0.59
D29 (D22)	22.2	28.8±0.2	615.4	387.1	0.63

*D means diameter and the number means the nominal diameter value

Table 2 Test variables

Specimen No.	Specimen ID	Ave. nominal diameter (mm)	Number of strands of fiber ribs	Measured pitch of fiber ribs (mm)	Number of samples
1	D19 (D16)-S6-P13.4	18.5	6	15.0	3
2	D19 (D16)-S6-P17.4	18.9	6	16.9	3
3	D19 (D16)-S6-P27.9	19.0	6	29.0	3
4	D19 (D16)-S10-P13.4	19.0	10	15.4	3
5	D19 (D16)-S10-P17.4	19.0	10	16.9	3
6	D19 (D16)-S10-P27.9	19.1	10	29.1	3
7	D25 (D19)-S10-P17.8	25.0	10	18.9	3
8	D25 (D19)-S10-P23.1	25.0	10	24.3	3
9	D25 (D19)-S10-P37.0	24.8	10	38.8	3
10	D25 (D19)-S14-P17.8	25.0	14	18.8	3
11	D25 (D19)-S14-P23.1	25.0	14	22.6	3
12	D25 (D19)-S14-P37.0	24.6	14	39.1	3
13	D29 (D22)-S12-P20.0	28.5	12	19.6	3
14	D29 (D22)-S12-P26.0	28.7	12	26.7	3
15	D29 (D22)-S12-P41.6	28.5	12	49.3	3
16	D29 (D22)-S16-P20.0	29.0	16	19.5	3
17	D29 (D22)-S16-P26.0	29.1	16	26.6	3
18	D29 (D22)-S16-P41.6	28.8	16	45.7	3
19	D19 (deformed steel)	19.1	-	13.4	3

Fig. 4 View of framework with GFRP Hybrid bar

A total of 63 specimens were tested, including three deformed steel bars (D19). Table 2 shows the test parameters, i.e., the number of fiber strands and the pitch of the fiber ribs. For the nominal diameter, the Average nominal diameter for the three deformed steel bars was used. The goal was to verify the mechanical resistance of the ribs with increasing density of the fiber ribs and with decreasing spacing between the fiber ribs. In order to increase the accuracy of the experimental results, three identical specimens were fabricated for each parameter. The pitch was obtained by measuring five points for each GFRP Hybrid bar. It was found that there was a slight discrepancy between the designed and measured pitch, with the measured pitch somewhat higher than the designed pitch. This was considered a fabrication discrepancy; in general, the tendency for the pitch to increase or decrease in terms of analysis of the bond behavior was valid. Bond strength was calculated as shown in Eq. (1). Bond stress is the surface stress of GFRP Hybrid bar along the bond length when tensile load acted. For diameter of GFRP Hybrid bar, outer diameter was considered. Failure load was determined in concrete splitting or pull-out failure at peak loading state.

$$\tau = \frac{p}{\pi d l} \tag{1}$$

where,

τ = bond stress at ultimate load of p (MPa)

p = peak load in failure (kN)

d = diameter of GFRP Hybrid bar or steel bar (mm)

l = bond length (mm)

A wooden framework was fabricated for the test specimens (Fig. 4). The embedment length was measured carefully from the bottom inside of the wooden frame. In order to avoid eccentricity during the concrete casting, the punctured in the very center of the concrete anchorage block and a thick plate was fixed at the free end of the GFRP Hybrid bar. Proper vibration was also provided, and the samples were cured for a few days in air.
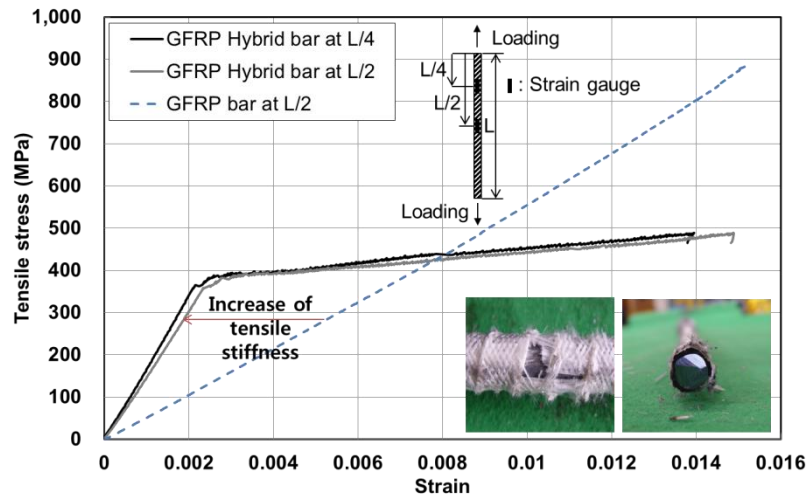
Fig. 5 Tensile stress-strain relationship

Table 3 Tensile properties of GFRP Hybrid bar of D19 (D16)

Test specimen No.	Tensile load (kN)	Tensile strength (MPa)	Modulus of elasticity (GPa)
1	138.4	483.0	160.4
2	140.7	490.9	147.6
3	125.6	438.4	149.8
4	140.7	490.9	152.6
5	135.5	472.7	150.0
Average		475.2	152.1
Standard deviation		19.6	-
Designed value		333.2*	152.1

* applied the environmental reduction factor of 0.8 for GFRP

3.2 Test specimens

The concrete used was normal-weight and ready-mix concrete with a target concrete cylinder strength of 27 MPa. Curing period was 30 days in air. In order to determine the property of concrete strength, nine cylindrical specimens with dimensions of 150 × 200 mm were fabricated and compressive failure test was carried out by the universal test machine (UTM).

The compressive strength test was conducted at the laboratory; the characteristic strength of the concrete was measured to be 25.3 ± 3.0 MPa. The materials properties of the E-glass fiber and vinyl ester resin were given in a previous study by You *et al.* (2007). For the fiber ribs, Kuralon™ filament provided by Kuraray Co. was used according to the designed number of strands of the

fiber ribs.

Fig. 4 and Table 3 show the results of the uniaxial tensile test of the D19 (D16) GFRP Hybrid bar, in which the outer portion was 19.1-mm-thick GFRP and the core section of the deformed steel bar was 15.9 mm thick. Tensile tests on the specimens were carried out in accordance with ASTM D 3916 (2002). The measured modulus of elasticity was obtained at the two points of L/2 and L/4 in compliance with CSA S806-12. The Average value was 152.1 GPa with a cross-sectional ratio of 0.48%. This is a excellent increase as compared to the pure GFRP bar, which had a modulus of elasticity of approximately 50 GPa. The Average tensile strength of the GFRP Hybrid bar was 475.5 MPa and the designed tensile strength was 333.2 MPa including the environmental reduction factor of 0.7. In terms of ductility behavior, the GFRP Hybrid bar exhibited good bi-linear stress–strain behavior, whereas the commercial bar showed typical linear behavior until failure. There was a significant discrepancy in stress–strain behavior between the hybrid bar and the conventional GFRP bar. As shown in Fig. 5, the GFRP Hybrid bar exhibited much higher structural stiffness than the conventional GFRP bar. Although the tensile strength was lower than that of the conventional GFRP bar due to a much lower volume fraction of glass fiber, it may be valid to resist the tensile strength under the service load.

3.3 Test setup, test procedure and measurements

The pull-out test was conducted according to ASTM D 7913. Fig. 6 shows the loading cage for the pull-out specimens and the linear variable differential transformer (LVDT) for slip measurements. The loading cage, designed to align the vertical line from the actuator to the GFRP Hybrid bar, was $300 \times 300 \times 700$ mm. It was fixed to the upper grip of the universal test machine (UTM) with a 100-mm-thick steel rod. This minimized eccentricity during the pull-out test. The loading cage was connected using a hinged connector to provide good alignment to the GFRP Hybrid bar with increasing pull-out loads. To measure the slip of the bar, one LVDT was installed at the center of the GFRP Hybrid bar at the bonded end. The concrete anchorage block was positioned on the center of a bearing plate 50 mm thick. The loading end of the GFRP Hybrid bar was passed through the hole at the center of the bearing plate. A UTM mechanical grip with a grip length of 100 mm was used in order to avoid premature slip. This grip length was insufficient to ensure the tensile failure of the GFRP Hybrid bar; however, the mechanical grip could provide the proper resistance until bond failure, including concrete splitting. The measurement of slip within the grip was conducted with visual inspection using two reference lines at the grip plate and reinforcement. This test was carried out using a 2,000 kN UTM, where the pull-out loading was automatically applied at a loading speed of 23 kN/min as specified by ASTM D 7913.

4. Results and discussions

4.1 Mode of failure resulted from bond test

Fig. 7 shows the failure mechanism of the deformed steel bar. The D16 and D19 deformed steel bars were governed by pull-out failure, whereas the D22 deformed steel bar showed concrete splitting failure. This is mainly due to the combined effect of longer bond length and higher shear strength, resulting in concrete crushing as a function of bar deformation.
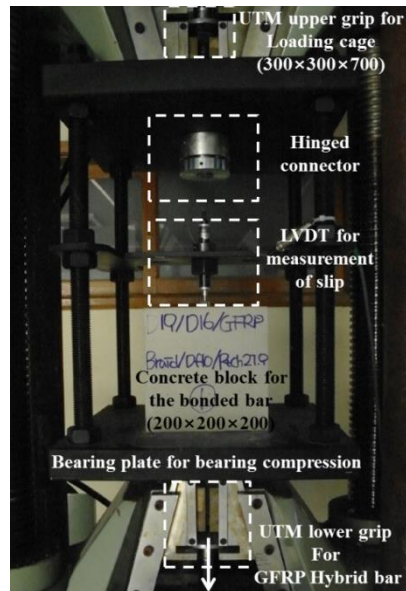
Fig. 6 Test set up and measurements (unit in mm)

The mode of failure for the GFRP Hybrid bar was in concrete splitting, as shown Fig. 8. This is mainly because the GFRP Hybrid bar had a lower modulus of elasticity than the deformed steel bar, such that the higher deformation of the GFRP Hybrid bar led to cracking until reaching the ultimate level of bond stress. Fig. 8(a) shows the interfacial bond failure of the GFRP Hybrid bar. The bond face might have moved along the loading direction more than the deformed steel bar due to its lower modulus of elasticity. The fiber ribs were slightly damaged at the surface level, hence, there was good transfer of the bond stress to the concrete. Visual inspection showed no evidence of slippage between the interfaces until the ultimate state.

(a) Pull-out failure   (b) Concrete splitting failure

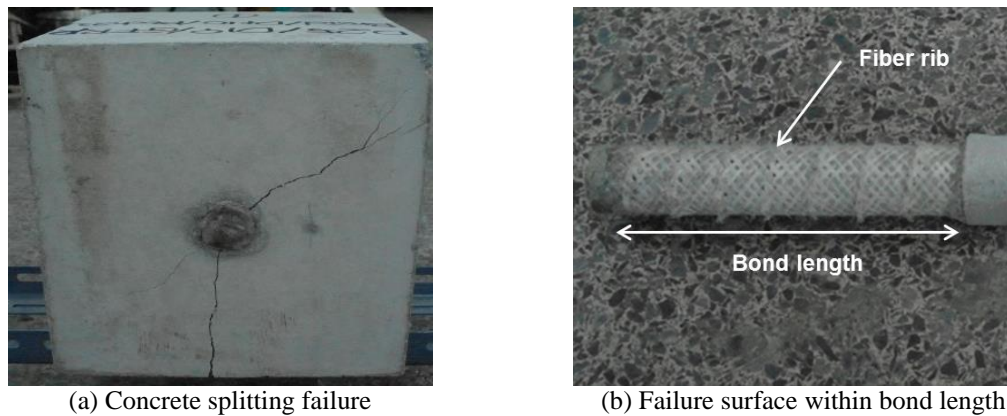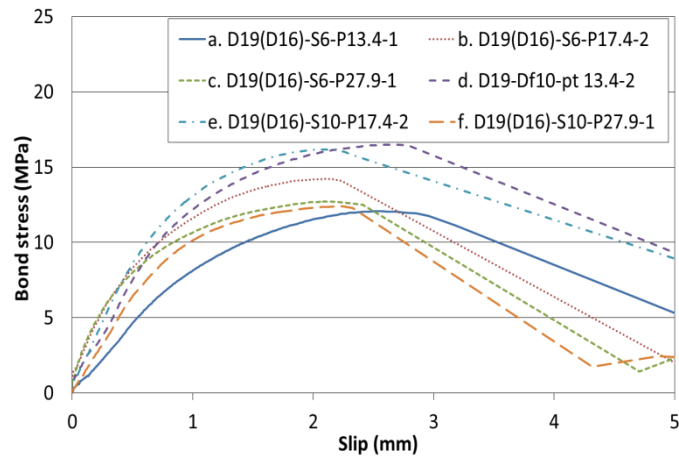Fig. 7 Interfacial bond failures for deformed steel bar specimen

(a) Concrete splitting failure   (b) Failure surface within bond length

Fig. 8 Interfacial bond failures for GFRP Hybrid bar specimen
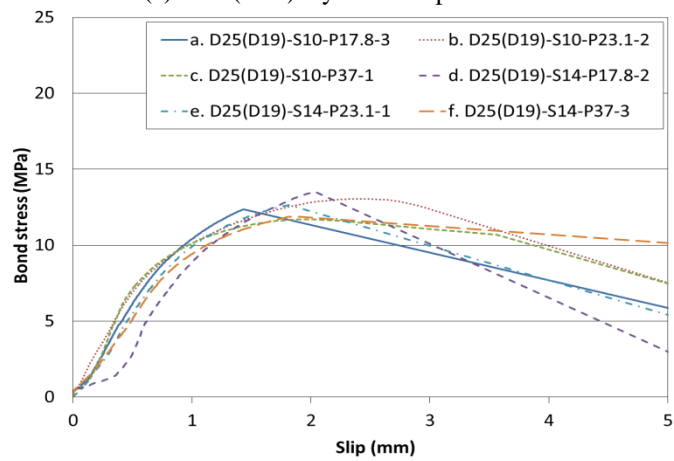
4.2 Bond stress-slip relationship

Fig. 9 shows the bond stress and slip curves of the GFRP Hybrid bar and the deformed steel bar. Bond strength was calculated by the equilibrium of forces. It was found that the bond strength decreased as the bar diameter increased. At the beginning of loading, there was no measurable slip because of chemical adhesion at the interface between the concrete and the bars. It was found that chemical adhesion of the deformed steel bar was much higher than that of the GFRP Hybrid bar. This is because the surface treatment of the steel bar was better in concrete as compared to the GFRP Hybrid bar. During the second stage up to ultimate load, the bond is due to mechanical interlocking. In this stage, micro-cracking propagated from the surface of the bar to the concrete cover. For the maximum slip at bond strength, the deformed steel bar showed higher slip as compared to the GFRP Hybrid bar as a result of the combined effect of poorer chemical adhesion and lower modulus of elasticity of the GFRP Hybrid bar.

If micro-cracking reaches the concrete cover, the bond strength between the bar and the concrete is sufficiently maintained and failure is governed by concrete splitting. If micro cracking does not reach the cover, the bond stress is exceeded when the peak stress is reached, at which point the slip increases and the load decreases. Thus, the sample fails by pull-out. At peak load, all the GFRP Hybrid bars failed in concrete splitting due to the sufficiently maintained shear strength between the GFRP Hybrid bar and concrete.
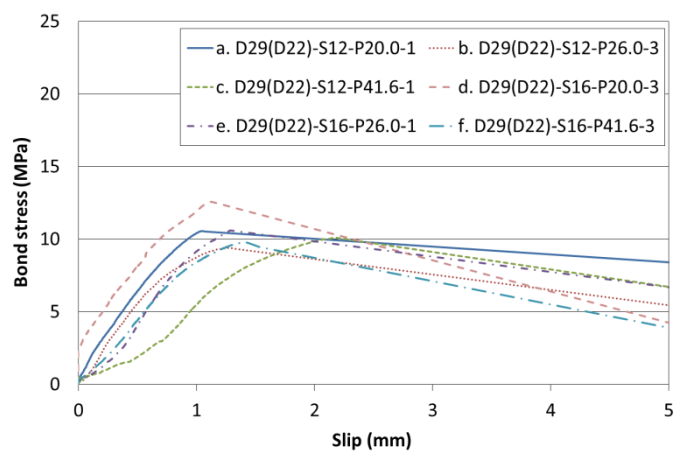
The bond strength and the failure mechanism of the test specimens are summarized in Table 3. Investigation revealed that the average bond strength varied according to the bar diameter, number of strands of fiber, and pitch between fiber ribs. The mode of failure of the GFRP Hybrid bar was concrete splitting. Concrete splitting in bond behavior occurs with the concrete cursing as a function of bar deformation. This can be explained using the average characteristic strain calculated from the stress–strain relationship by Hooke's Law. The average modulus of elasticity of the GFRP Hybrid bar was used with 152.1 MPa of D19 (D16) for relative comparison. As compared to the deformed steel bar, the strain was 103 times higher. This larger deformation behavior led to significant cracking; hence, the mode of failure of the GFRP Hybrid bar was concrete splitting, whereas most of the deformed steel bars exhibited pull-out failure resulting from interfacial damage by much less strain behavior.

(a) D19 (D16) Hybrid bar specimens

(b) D25 (D19) Hybrid bar specimens

(c) D29 (D22) Hybrid bar specimens

Fig. 9 Bond stress-slip relationship

Table 3 Bond test results

Specimen No.	Test No.	Failure load (kN)	Slip (mm)	Ave. failure load (kN)	Ave. characteristic strain	Ave. bond strength (MPa)	Ave. slip (mm)	Mode of failure
1	1	74.5	2.6	74.2	0.00182	13.5	3.0	Concrete splitting
	2	75.5	3.5					Concrete splitting
	3	72.5	2.8					Concrete splitting
2	1	83.1	2.5	81.9	0.00193	14.5	2.4	Concrete splitting
	2	80.1	2.4					Concrete splitting
	3							Concrete splitting
3	1	71.6	2.2	72.0	0.00168	12.7	2.2	Concrete splitting
	2	72.3	2.2					Concrete splitting
	3							Concrete splitting
4	1	92.8	1.6	94.2	0.00220	16.2	2.3	Concrete splitting
	2	93.9	2.8					Concrete splitting
	3	95.9	2.6					Concrete splitting
5	1	90.1	2.3	90.7	0.00209	16.0	2.2	Concrete splitting
	2	91.2	2.1					Concrete splitting
	3							Concrete splitting
6	1	70.6	2.2	72.7	0.00168	12.8	2.3	Concrete Splitting
	2	77.9	2.5					Concrete Splitting
	3	69.6	2.2					Concrete Splitting
7	1	125.9	3.4	123.6	0.00165	12.6	2.7	Concrete Splitting
	2							Concrete Splitting
	3	121.2	1.9					Concrete Splitting
8	1	97.9	3.2	109.0	0.00146	11.1	3.1	Concrete splitting
	2	129.1	2.7					Concrete splitting

<div align="center">Continued-</div>

	3	100.1	3.5					Concrete splitting
9	1	113.9	1.9	112.1	0.00152	11.5	2.2	Concrete Splitting
	2	110.8	2.2					Concrete Splitting
	3	111.5	2.6					Concrete Splitting
10	1	114.2	1.6	125.6	0.00168	12.8	1.8	Concrete Splitting
	2	132.7	2.0					Concrete Splitting
	3	130.0	1.8					Concrete Splitting
11	1	132.1	1.8	118.9	0.00159	12.1	2.5	Concrete Splitting
	2	93.9	3.4					Concrete Splitting
	3	130.7	2.4					Concrete Splitting
12	1				0.00160			Concrete Splitting
	2							Concrete Splitting
	3	115.4	1.9	115.4		12.0	1.9	Concrete Splitting
13	1	140.4	10.3	140.4	0.00144	10.8	1.1	Concrete Splitting
	2							Concrete Splitting
	3							Concrete Splitting
14	1	125.6	1.5	123.8	0.00126	9.5	1.3	Concrete Splitting
	2	122.4	1.1					Concrete Splitting
	3	123.5	1.3					Concrete Splitting
15	1	131.7	2.2	132.2	0.00136	10.2	2.2	Concrete Splitting
	2	146.4	2.5					Concrete Splitting
	3	118.6	2.0					Concrete Splitting
16	1	152.7	1.3	154.2	0.00153	11.7	1.3	Concrete splitting
	2	143.3	1.3					Concrete Splitting
	3	166.6	1.4					Concrete Splitting
17	1	140	1.3	129.5	0.00128	9.8	1.4	Concrete Splitting
	2	106.2	1.3					Concrete Splitting

Continued-

	3	142.2	1.6					Concrete Splitting
18	1	106.5	1.1	119.9	0.00121	9.1	1.5	Concrete Splitting
	2	124.4	1.8					Concrete Splitting
	3	128.8	1.5					Concrete Splitting
19	1	123.9	1.9	125.5	0.0022×10^{-3}	22.0	1.8	Pull-out
	2	129.7	1.5					Pull-out
	3	122.8	2.1					Concrete Splitting

4.3 Bond strength according to varying the number of strands and the pitch fiber ribs

In this study, a new GFRP Hybrid bar with a core section of deformed steel bar was developed. From this study, the effect of the fabrication details on the bond strength was investigated, and some improvements to enhance the bond strength were discussed. Fig. 10 shows the effect of varying the diameter, number of fiber strands, and pitch of the fiber ribs on the bond strength. For the D19 (D16) bar specimens, the bond strength increased as the number of strands increased, whereas increasing pitch decreased the bond strength, showing a significant drop for the specimen with a pitch of 27.9 mm. Investigation revealed that an increase in the number of strands of fiber is good for enhancing the bond strength, and the pitch guaranteed the bond strength of D19 (D16) bar specimens may be around 13.4 mm. For the D25 (D19) and D29 (D22) bar specimens, the bond strength was not significantly affected by the number of strands or the pitch of the fiber ribs. These results indicate that it can be cost effective to reduce the number of strands of fiber ribs and widen the pitch of fiber ribs for GFRP Hybrid bars with large diameters.

5. Comparative study using code equations of ACI 440 1R-15 and CSA S806-12

Various bond formulas, including some empirical equations, were developed for evaluating the bond performance and predicting the bond strength. For designing GFRP bars, there are two representative code equations, ACI440 1R-15 and the Canadian specification, CSA S806-12. In this study, the tested bond strength of the GFRP Hybrid bar was compared to the bond strength calculated by the two codes. For a straight bar, ACI440 1R-15 showed linear regression of the normalized average bond stress versus the normalized cover and embedment length, which resulted in the following relationship after rounding the coefficients. It was shown as equal to Eq. (2).

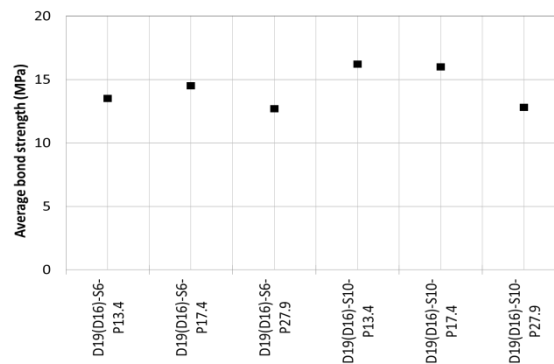$$\frac{u}{0.083\sqrt{f_c{'}}} = 4.0 + 0.3\frac{c}{d_b} + 100\frac{d_b}{l_e} \tag{2}$$

where,
u = stress acting on the surface of the bar (MPa)
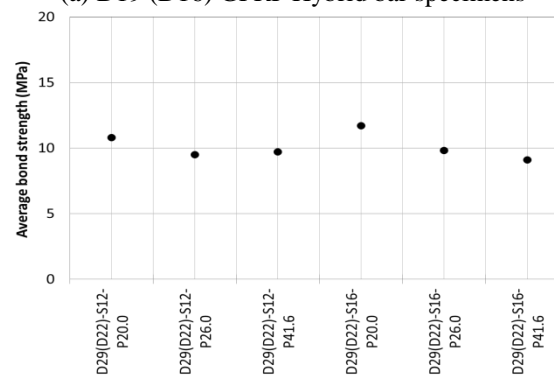$f_c{`}$ = characteristic strength of concrete (MPa)
d_b = Average nominal diameter (mm)
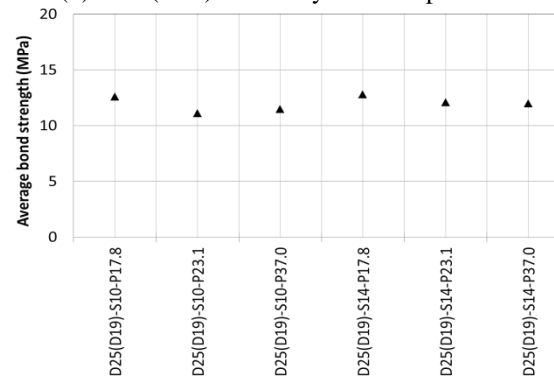l_e = embedment length for designed diameter of GFRP Hybrid bar (mm)

C = lesser of d_c (thickness of concrete cover measured from extreme tension fiber to center of bar)
or
$d_{c,side}$ (thickness of concrete cover measured from side face of member to center of longitudinal bar)
or
one-half of the center on center spacing of the bar (mm).

(a) D19 (D16) GFRP Hybrid bar specimens

(b) D25 (D19) GFRP Hybrid bar specimens

(c) D29 (D22) GFRP Hybrid bar specimens

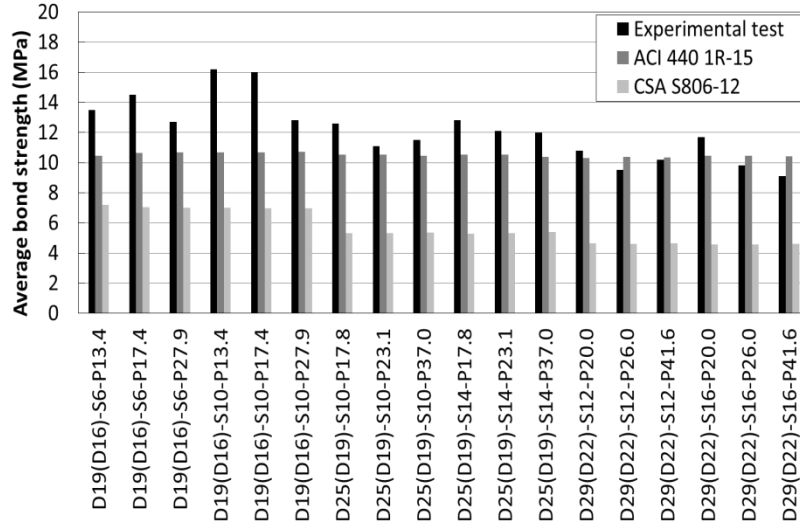Fig. 10 Effect of varying diameter, number of strands and pitch of fiber ribs

Fig. 11 Comparative results of bond equations with the bond test of GFRP Hybrid bar

CSA S806-12 is introduced as follows. Eq. (3) is reformulated for bond strengths from the equation of development length of bars in tension. Unlike the ACI440 1R-15 equation, the Canadian equation is based on the equilibrium of forces, and some environmental factors are applied. Both the ACI440 1R-15 and the CSA S806-12 equations consider the concrete compression as the square root term.

$$\tau_f = \frac{d_{cs}\sqrt{f_c{'}}}{1.15(k_1 k_2 k_3 k_4 k_5)\pi d_b} \tag{3}$$

where,
d_{cs} = distance from the closest concrete surface to the center of the bar being developed (shall not be greater than $2.5d_b$)
$f_c{}^`$ = specified compressive strength of concrete (MPa) (shall not be greater than 5MPa)
k_1 = bar location factor (1.0 for other cases)
k_2 = concrete density factor (1.0 for normal density concrete)
k_3 = bar size factor (1.0 for $A_b > 300$ mm^2)
k_4 = bar fiber factor (1.0 for CFRP and GFRP)
k_5 = bar surface profile factor (1.05 for ribbed surfaces)

Fig. 11 shows the comparative results of the ACI440 1R-15 and CSA S806-12 equations to the bond test results. The ACI440 1R-15 equation underestimates the bond strength for the D19 (D16) and D25 (D19) bar specimens, whereas it overestimates the bond strength for the group with the largest diameter, D29 (D22). On the other hand, the CSA S806-12 equation consistently underestimates the bond strength for all diameters, and its results are considerably safe region. The noticeable point is that the CSA S806-12 equation is more influenced by the varying diameters of the bar than the ACI440 1R-15 equation, showing decreased bond strength as the diameter of the

bar increases. The ACI440 1R-15 equation is regarded as more suitable for the bond strength prediction of GFRP Hybrid bars than the CSA S806-12 equation. However, there is some discussion about specimens No. 2, 4, 5, and 8 from Table 2, which shows relatively high bond strengths among the specimens. The high bond strength may be the result of an interlocking mechanism according to the concrete properties.

6. Conclusions

This study presents innovative research to develop a smart GFRP Hybrid bar. The smart GFRP Hybrid bar can enhance the modulus of elasticity as compared to conventional GFRP bars. Additionally, it can also promise superior durability against corrosion as compared to conventional steel bars. To verify the mechanical performance in terms of structural reinforcement, a fundamental study of the bond test was conducted. The variables were the bar diameter, the number of fiber strands, and the pitch of the fiber ribs.

- Investigation of the tensile strength revealed that the Average value was 152.1 GPa with a cross-sectional ratio of 0.48%. This is a excellent increase as compared to the pure GFRP bar (50 GPa). The stress–strain curve was bi-linear, such that ductile performance could be obtained, whereas the conventional GFRP bar was governed by linear behavior until reaching the ultimate state. However, the Average tensile strength must be enhanced by varying the cross-sectional ratio.
- All of test specimens of the GFRP Hybrid bar failed in concrete splitting. This was due to crack propagation resulting from deformation of the bar. The main reason for these results is the relatively low modulus of elasticity as compared to a conventional steel bar. The chemical adhesion at the initial loading stage was very low. The combination of the low modulus of elasticity and chemical adhesion may have led to significant slip during the pull-out loading. Special surface treatment of the GFRP Hybrid bar should be studied.
- In terms of the effect of varying diameter, number of fiber strands, and pitch of the fiber ribs on the bond strength, D19 (D16) showed increased bond strength with increasing number of strands, and the pitch guaranteed the bond strength of D19 (D16) bar specimens may be around 13.4 mm. For the D25 (D19) and D25 (D19) bar specimens, the bond strength was not significantly affected by the number of strands or the pitch of the fiber ribs. Thus, it is concluded that for cost effectiveness, reducing the number of strands of fiber and widening the pitch of the fiber ribs for large-diameter GFRP Hybrid bars may be a good strategy for fabrication.
- For comparative study using the two representative code equations, the ACI 440 1R-15 equation is regarded as more suitable for predicting the bond strength of GFRP Hybrid bars than the CSA S806-12 equation. The CSA S806-12 prediction was too conservative for evaluating the bond strength of GFRP Hybrid bars and it was largely influenced by the bar diameter. For further study, various geometrical and material properties such as concrete cover, cross-sectional ratio, and surface treatment should be considered. It can be verified that GFRP Hybrid bars can ensure the stronger durability of concrete structures.

Acknowledgments

References

AASHTO (2009), *LRFD Bridge Design Guide Specifications for GFRP-Reinforced Concrete Bridge Decks and Traffic Railings*, American Association of State Highway and Transportation Officials, Washington, DC, USA.

ACI Committee 440 (2015), *Guide for the Design and Construction of Concrete Reinforced with FRP Bars (ACI 440.1R-15)*, American Concrete Institute, Farmington Hills, MI, USA.

ASTM D 3916 (2008), *Standard Test Method for Tensile Properties of Pultruded Glass Fiber Reinforced Plastic Rods*.

ASTM D 7913 (2014), *Standard Test Method for Bond Strength of Fiber-Reinforced Polymer Matrix Composite Bars to Concrete by Pullout Testing*.

CAN/CSA S806-12 (2012), *Design and Construction of Building Structures with Fibre-Reinforced Polymers*, Canadian Standards Association/National Standard of Canada, Ontario, Canada.

Castro, P.F. and Carino, N.J. (1998), "Tensile and nondestructive testing of FRP bars", *J. Compos. Constr.*, **2**(1), 283-298.

Etman, E.E.S. (2011), "Innovative hybrid reinforcement for flexural members", *J. Compos. Constr.*, **15**(1), 2-8.

Islam, S., Afefy, H.M., Sennah, K. and Azimi, H. (2015), "Bond characteristics of straight- and headed-end, ribbed-surface, GFRP bars embedded in high-strength concrete", *Construct. Build. Mater.*, **83**, 283-298.

Kuralon™ filament, Kuraray Co. Ltd. http://www.kuraray.co.jp/.

Lau, D. and Pam, H.J. (2010), "Experimental study of hybrid FRP-reinforced concrete beams", *Eng. Struct.*, **32**(12), 3857-3865.

Mazaheripour, H., Barros, J.A., Sena-Cruz, J.M., Pepe, M. and Martinelli, E. (2013), "Experimental study on bond performance of GFRP bars in self-compacting steel fiber reinforced concrete", *Compos. Struct.*, **95**, 202-212.

Pecce, M., Manfredi, G., Realfonzo, R. and Cosenza, E. (2001), "Experimental and analytical evaluation of bond properties of GFRP bars", *J. Mater. Civ. Eng.*, **13**(4), 282-290.

Qu, W., Zhang, X. and Huang, H. (2009), "Flexural behavior of concrete beams reinforced with hybrid GFRP and steel bars", *J. Compos. Constr.*, **13**(5), 350-359.

S807-02 (2010), *Specification for Fiber-Reinforced Polymers*, Canadian Standard Association.

Seo, D.W., Park, K.T., You, Y.J. and Kim, H.Y. (2013), "Enhancement in elastic modulus of GFRP bars by material hybridization", *Scientific Research:Engineering*, **5**(11), 865-869.

Tastani, S.P. and Pantazopouou, S.J. (2006), "Bond of GFRP bars in concrete: experimental study and analytical interpretation", *J. Compos. Constr.*, **10**(5), 381-391.

Tighiouart, B., Benmokrane, B. and Gao, D. (1998), "Investigation of bond in concrete member with fibre-reinforced polymer (FRP) bars", *Constr. Build. Mater.*, **12**(8), 453-462.

Xue, W., Zheng, Q., Yang, Y. and Fang, Z. (2014), "Bond behavior of sand-coated deformed glass fiber reinforced polymer rebars", *J. Reinf. Plast. Compos.*, **33**(10), 895-910.

You, Y.J., Park, Y.H., Kim, H.Y. and Park, J.S. (2007), "Hybrid effect on tensile properties of FRP rods with various material compositions", *Compos. Struct.*, **80**(1), 117-122.